Measurement of Ll, $L\alpha$, $L\beta$, and $L\gamma$ x-ray production cross sections in rare-earth elements by 60-keV photons

K. S. Mann, Raj Mittal, K. L. Allawadhi, and B. S. Sood
Nuclear Science Laboratories, Physics Department, Punjabi University, Patiala 147 002 India
(Received 12 December 1990)

Our earlier measurements [Shatindra, Allawadhi, and Sood, Phys. Rev. A **31**, 2918 (1985)] of Ll, $L\alpha$, $L\beta$, and $L\gamma$ x-ray production cross sections in elements with $73 \leq Z \leq 92$ by 60-keV photons have been extended to 11 rare-earth elements in the range $57 \leq Z \leq 68$ in order to examine enhancement in L-subshell x-ray production due to transfer of vacancies from the K to the L shell. The measured values of absolute cross sections have been interpreted in terms of K-shell photoelectric cross sections, probabilities of $K \rightarrow L$ radiative and nonradiative transitions, L-subshell photoelectric cross sections, fluorescence yields, Coster-Kronig transition probabilities, and radiative decay rates. Fairly good agreement between the experimental and calculated values indicates indirectly the correctness of the theoretical calculations of the atomic parameters in terms of which the experimental results have been interpreted.

I. INTRODUCTION

Earlier, we have measured [1] Ll, $L\alpha$, $L\beta$, and $L\gamma$ x-ray production cross sections by 59.57-keV photons in high-Z elements, $73 \leq Z \leq 92$, with K-edge energies higher than 59.57 keV. We extend the measurements to intermediate elements $57 \leq Z \leq 68$ with K-edge energies lower than 59.57 keV in order to demonstrate that when K-shell electrons are also ionized in addition to L- M-, and higher-shell electrons and when the mean lifetime of K-shell vacancies is shorter than that of L-shell vacancies, the intensities of L-shell x-ray emission lines are considerably enhanced. The enhancement in the L-shell x-ray emission intensity is due to the addition in the vacancies created initially by direct photoionization of various L-subshell electrons. This ionization occurred through the transfer of vacancies from the K shell to various L subshells through radiative and nonradiative transitions, depending upon the selection rules, prior to L x-ray emission.

II. METHOD OF MEASUREMENTS AND RESULTS

The method of measurement, as described earlier [2], consists of irradiating a target of known composition and thickness with a predetermined flux of 59.57-keV γ rays from a ^{241}Am source in a 90° single-reflection geometrical setup [3]. The absolute yield of L x rays under the Ll, $L\alpha$, $L\beta$, and $L\gamma$ peaks of the emission spectrum was measured with a calibrated Si(Li) x-ray spectrometer. The ^{241}Am source (model AMC 24) of approximately 14 mCi strength was purchased from Radio Chemical Center, England. Self-supporting targets of La, Ce, Pr, Nd, Sm, Eu, Gd, Tb, Dy, Ho, and Er were made from their oxides by the technique described earlier [4] but the metallic target of Gd was purchased from Reactor Experiments, Inc., U.S.A. L x rays emitted from the targets were analyzed with an ORTEC Si(Li) detector with an active diameter of 10 mm and sensitive crystal depth of 4.66 mm and a Be window of 0.0254 mm thickness coupled to an ND-600 multichannel analyzer, having a resolution of approximately 170 eV at 5.9 keV. The values of the effective detector efficiency and the correction factors due to attenuation of the incident γ rays before their interaction in the target and the emitted L x rays along their path prior to absorption in the detector sensitive volume, that are needed in the present measurements, were determined experimentally by the method previously described [1]. The measurements of cross sections for Gd were made using targets of seven different thicknesses and the results were found to agree with one another within experimental uncertainties. Typical results for the $L\alpha$ line are shown in Fig. 1. The independence of the cross sections of the target thickness confirms that the corrections applied for the attenuation of the incident γ rays before the interaction and emitted x rays after the interaction in the target are correct. It also shows that in the present measurements the contribution of K x rays produced in the target by incident γ rays towards further additional emission of L x rays is not of much significance. If the contribution due to ionization of L-shell electrons by K x rays produced in the target was

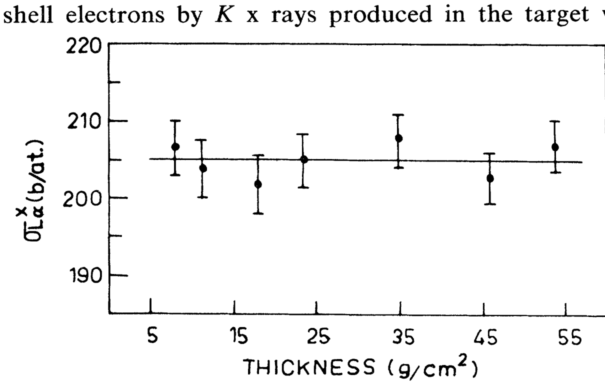

FIG. 1. Plot of $L\alpha$ x-ray production cross sections in Gd against target thickness.

TABLE I. Comparison of the present measurements of Ll, $L\alpha$, $L\beta$, and $L\gamma$ x-ray production cross sections in elements $57 \le Z \le 68$ by 60-keV photons with calculated values. EF denotes enhancement factor.

Element	σ_{Ll}^{x} (b/at.) Obs.	Calc.[a]	Calc.[b]	EF[c]	$\sigma_{L\alpha}^{x}$ (b/at.) Obs.	Calc.[a]	Calc.[b]	EF[c]
La	3.4±0.3	3.7	0.37	9.2	98±7	97	9.8	10.0
Ce	4.3±0.3	4.2	0.43	10.0	107±7	110	11.3	9.4
Pr	4.8±0.4	4.8	0.50	9.6	149±9	124	12.6	9.4
Nd	5.5±0.4	5.3	0.58	9.5	139±9	138	15.1	9.2
Sm	6.8±0.5	6.7	0.76	9.0	175±11	170	19.3	9.1
Eu	7.8±0.6	7.5	0.87	9.0	186±12	189	22.0	8.5
Gd	8.3±0.6	8.4	0.99	8.4	205±14	208	24.8	8.3
Tb	9.8±0.8	9.5	1.16	8.5	234±14	230	28.1	8.3
Dy	10.0±0.8	10.7	1.33	7.5	256±15	256	31.8	8.1
Ho	12.0±1.0	11.9	1.45	8.3	294±18	281	36.5	8.1
Er	14.5±1.0	13.3	1.71	8.5	303±20	311	40.1	7.6

Element	$\sigma_{L\beta}^{x}$ (b/at.) Obs.	Calc.[a]	Calc.[b]	EF[c]	$\sigma_{L\gamma}^{x}$ (b/at.) Obs.	Calc.[a]	Calc.[b]	EF[c]
La	76±5	73	14.4	5.3	10±1	10.5	2.8	3.6
Ce	85±5	83	16.5	5.2	11±1	12.0	3.2	3.6
Pr	99±6	95	18.8	5.3	13±1	13.3	3.6	3.5
Nd	107±7	105	21.2	5.1	16±1	15.0	4.1	3.9
Sm	130±9	131	27.2	4.8	20±2	19.2	5.3	3.8
Eu	150±11	146	30.8	4.8	20±2	21.6	6.0	3.3
Gd	161±12	163	34.8	4.6	21±2	24.0	6.8	3.1
Tb	185±13	181	39.1	4.7	27±2	27.0	7.6	3.5
Dy	194±13	203	42.8	4.5	28±2	30.5	8.2	3.4
Ho	230±14	226	50.2	4.5	35±3	34.0	9.7	3.5
Er	250±17	252	56.6	4.4	42±3	38.0	11.1	3.8

[a]Calculated values using relations (1)–(4) given in text.
[b]Calculated values using relations (1)–(4) when $n_{KL_i}=0$.
[c]Enhancement factor, which is equal to the ratio of the observed cross section to the value given under Calc.[b].

significant, thicker targets would have yielded higher values of cross sections due to additional contributions to L x-ray production.

The measured values of Ll, $L\alpha$, $L\beta$, and $L\gamma$ cross sections are compared in Table I with those calculated from the following relations:

$$\sigma_{Ll}^{x}=[\sigma_3+\sigma_K n_{KL_3}+(\sigma_2+\sigma_k n_{KL_2})f_{23}+(\sigma_1+\sigma_K n_{KL_1})(f_{13}+f_{12}f_{23})]\omega_3 F_{3l}\ , \quad (1)$$

$$\sigma_{L\alpha}^{x}=[\sigma_3+\sigma_K n_{KL_3}+(\sigma_2+\sigma_K n_{KL_2})f_{23}+(\sigma_1+\sigma_K n_{KL_1})(f_{13}+f_{12}f_{23})]\omega_3 F_{3\alpha}\ , \quad (2)$$

$$\sigma_{L\beta}^{x}=(\sigma_1+\sigma_K n_{KL_1})\omega_1 F_{1\beta}+[(\sigma_2+\sigma_K n_{KL_2})+(\sigma_1+\sigma_K n_{KL_1})f_{12}]\omega_2 F_{2\beta}+[(\sigma_3+\sigma_K n_{KL_3})+(\sigma_2+\sigma_K n_{KL_2})f_{23}+(\sigma_1+\sigma_K n_{KL_1})(f_{13}+f_{12}f_{23})]\omega_3 F_{3\beta}\ , \quad (3)$$

$$\sigma_{L\gamma}^{x}=(\sigma_1+\sigma_K n_{KL_1})\omega_1 F_{1\gamma}+[(\sigma_2+\sigma_K n_{KL_2})+(\sigma_1+\sigma_K n_{KL_1})f_{12}]\omega_2 F_{2\gamma}\ , \quad (4)$$

TABLE II. Measured values of the coefficients a_n ($n=0,1,2,3,4$) corresponding to the Ll, $L\alpha$, $L\beta$, and $L\gamma$ groups of L x rays.

Group of L x rays	a_0	a_1	a_2	a_3	a_4
Ll	11 803	−793	20	-22.27×10^{-2}	93.15×10^{-5}
$L\alpha$	44 913	−2830	67	-70.49×10^{-2}	28.15×10^{-15}
$L\beta$	−11 885	591	-97.59×10^{-1}	51.94×10^{-3}	35.40×10^{-6}
$L\gamma$	126 996	−8316	204	-22.22×10^{-1}	90.67×10^{-4}

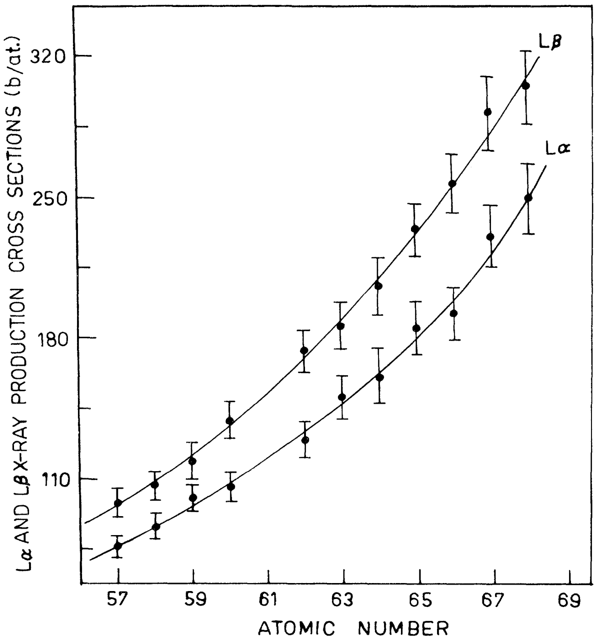

FIG. 2. $L\alpha$ and $L\beta$ x-ray production cross sections in different elements with atomic number $57 \leq Z \leq 68$ by 59.57-keV photons. ⧫: measured cross sections; solid curve: fitted curve drawn with measured a_n ($n = 0,1,2,3,4$) coefficients.

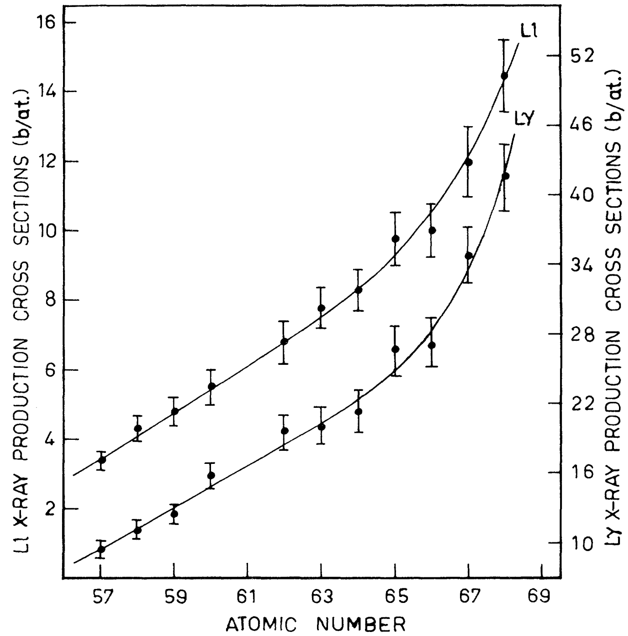

FIG. 3. Ll and $L\gamma$ x-ray production cross sections in different elements with atomic number $57 \leq Z \leq 68$ by 59.57-keV photons. ⧫: measured cross sections; solid curve: fitted curve drawn with measured a_n ($n = 0,1,2,3,4$) coefficients.

where σ_K and σ_1, σ_2 and σ_3 are the K and L subshell photoionization cross sections [5]; ω_1, ω_2, and ω_3 are the L-subshell fluorescence yields [6]; f_{ij} are Coster-Kronig transition probabilities from the i to j subshells [6]; F_{3l} is the fraction [7] of L x rays originating from the L_3 transition that contribute to the Ll peak. All other F's are similarly defined. n_{KL_i} corresponds to the number of additional vacancies transferred to the L_i subshell from the K shell through radiative $n_{KL_i}(R)$ and nonradiative $n_{KL_i}(A)$ transitions [8]:

$$n_{KL_i} = n_{KL_i}(R) + n_{KL_i}(A) .$$

The uncertainties in the measured cross sections are 6–8 % and are due to counting statistics and errors involved in the determination of various parameters relating to the flux of photons incident on the target, detection efficiencies, and other correction factors for the attenuation of the incident γ rays and emitted x rays needed for the measurement of cross sections. A fairly good agreement between experimental and calculated values indicates indirectly the accuracy of the values of atomic parameters used in the calculations for the cross sections. Cross sections calculated from relations (1)–(4) by setting $n_{KL_i} = 0$ in them, i.e., assuming that there is no K to L transfer of vacancies prior to L x-ray emission, are also shown in the third column of Table I. Ratios of the experimental cross sections with those calculated on the assumption of no transfer of K to L_i vacancies give the enhancement factors and are listed in the fourth column of Table I. It may be noted that all four groups of L x-ray emission lines, namely Ll, $L\alpha$, $L\beta$, and $L\gamma$, are enhanced due to the transfer of vacancies from the K to L subshell, but the enhancement in the Ll and $L\alpha$ groups of lines resulting from transitions to the L_3 subshell only is much greater than that for the $L\beta$ and $L\gamma$ groups, which contain predominantly lines resulting from L_1 and L_2 subshells, indicating that most of the vacancies in the K shell are transferred to L_3 subshell.

The observed cross sections are fitted to the relation

$$\sigma^x_{L_i} = \sum_{n=1}^{n} a_n Z^n . \tag{5}$$

The values of the coefficients a_n are listed in Table II. Agreement of the experimental values of cross sections with the fitted curves as shown in Figs. 2 and 3 proves that relation (5) may be used to determine the cross sections for the emission of various L x-ray groups, from different intermediate Z elements, by 60-keV γ rays which are often used to excite fluorescent x rays for trace elemental analysis of samples using the x-ray fluorescence technique.

ACKNOWLEDGMENT

Financial assistance from the Department of Science and Technology (Government of India) and University Grants Commission (India) is gratefully acknowledged.

[1] K. Shatendra, K. L. Allawadhi, and B. S. Sood, Phys. Rev. A **31**, 2918 (1985).
[2] S. K. Arora, K. L. Allawadhi, and B. S. Sood, J. Phys. B **13**, 3157 (1980).
[3] S. K. Arora, K. L. Allawadhi, and B. S. Sood, Phys. Rev. A **23**, 1147 (1981).
[4] M. I. Singh and B. S. Sood, Nuovo Cimento B **8**, 261 (1972).
[5] J. H. Scofield, Lawrence Livermore National Report No. UCRL-51326, 1973 (unpublished).
[6] M. O. Krause, J. Phys. Chem. Ref. Data **8**, 307 (1979).
[7] J. H. Scofield, At. Data Tables **14**, 121 (1974).
[8] P. Venugopala Rao, M. H. Chen, and X. Crasemann, Phys. Rev. A **5**, 997 (1972).